J Electroceram (2009) 23:497–501
DOI 10.1007/s10832-008-9518-y

Electrical and optical properties of epitaxial and polycrystalline undoped and Al-doped ZnO thin films grown by pulsed laser deposition

Jun Hong Noh · Jae-Sul An · Jin Young Kim · Chin Moo Cho · Kug Sun Hong · Hyun Suk Jung

Received: 31 May 2007 / Accepted: 25 April 2008 / Published online: 17 May 2008
© Springer Science + Business Media, LLC 2008

Abstract Undoped and Al-doped (1.6%) ZnO films were prepared on (0001) sapphire and fused silica substrates using a pulsed laser deposition technique. The ZnO films on sapphire substrates were epitaxially grown, while the ZnO films on fused silica substrates were texturally grown. The films on sapphire substrates were ordered along the in-plane direction and had grains in which the *c*-axis was well aligned normal to the substrate. However, the films on fused silica were randomly oriented along the in-plane direction and had poor c-axial aligned grains. The structure analyses showed that the epitaxial ZnO films had low-angle grain boundaries, while the textured polycrystalline ZnO films had high-angle tilt and twist grain boundaries. The nature of the grain boundaries influenced the electrical and optical properties of the undoped and Al-doped ZnO films. Resistivity, Hall mobility, carrier concentration, and near band edge emission of the films were measured at room temperature and discussed in connection with the nature of grain boundaries.

Keywords Al-doped ZnO · Thermal stability · Epitaxial · Polycrystalline · Grain boundary · Transparent conducting oxide

J. H. Noh · J.-S. An · J. Y. Kim · C. M. Cho · K. S. Hong (✉)
School of Materials Science & Engineering,
Seoul National University,
Seoul 151-744, South Korea
e-mail: kshongss@plaza.snu.ac.kr

H. S. Jung
School of Advanced Materials Engineering, Kookmin University,
Jeongneung-dong, Seongbuk-gu,
Seoul 136-702, South Korea

1 Introduction

Zinc oxide (ZnO) is an interesting material for optoelectronic devices because of its direct wide band gap (3.3 eV), the strongest bond strength within the II–VI semiconductor family, and a very large exciton binding energy of 60 meV [1]. Therefore, characterization of the electrical and optical properties of the ZnO film is important and has been studied previously [2–5]. ZnO is an n-type semiconductor due to intrinsic defects such as oxygen vacancies and zinc interstitials. In particular, the heavily doped ZnO film with a carrier concentration of approximately 10^{20} cm^{-3} has been investigated for use as a transparent conduction oxide (TCO) [6].

Al-doped ZnO thin films, among heavily doped ZnO thin films prepared by various depositional techniques, have attracted considerable interest because of their low resistivity and high transmittance in the visible region [6–8]. Among the various methods, pulsed laser deposition (PLD) is a process with advantages of high quality crystalline and epitaxial growth over other techniques [9, 10]. The electrical properties of as-deposited Al-doped ZnO thin films grown on sapphire and fused silica substrates by PLD have been previously reported [11, 12]. However, most studies have focused on the electrical and optical properties of the as-deposited films, while little attention has been paid to thermal stability. The electrical properties after air annealing should be investigated, since the thermal stability of TCO is essential for real devices in which process accompanies air annealing [13].

In this study, undoped ZnO and Al-doped ZnO thin films were prepared by PLD on (0001) sapphire and fused silica substrates. The structure of the films on each substrate was studied, and the thermal stability of electrical properties after air annealing at 450 °C was investigated in connection

with the nature of grain boundaries. In addition, the photoluminescence of each film was investigated at room temperature.

2 Experimental procedure

ZnO and Al-doped (1.6%) ZnO targets were made through a conventional power mixed method using ZnO (99.99%) and Al_2O_3 (99.99%) powders. The undoped and Al-doped ZnO films were grown on fused silica and (0001) sapphire substrates using a pulsed laser deposition technique with a KrF laser (λ=248 nm). The substrates were kept at a temperature of 400 °C, during deposition, which was performed under 100 mTorr of pure oxygen. The deposited films were cooled to room temperature with a cooling rate of 10 °C/min. The distance between the target and the substrate was 5 cm, the deposition rate was 3 Hz, and the energy density was 2 J/cm^2.

The structural analyses such as θ–2θ scan, rocking curve, and pole figure of the films were done by X-ray diffraction (XRD; X'Pert Phillips XRD system, Cu target). Resistivity, Hall mobility, and the carrier concentration of the films were measured at room temperature in a van der Pauw configuration by Hall measurement. Surface roughness of the films was measured using atomic force microscopy (AFM). Photoluminescence was excited by a 325-nm He–Cd laser and measured at room temperature.

3 Results and discussion

The θ–2θ XRD spectra of the as-deposited and air-annealed undoped ZnO (ZnO) and Al-doped ZnO (AZO) thin films grown on (0001) sapphire and fused silica substrates are shown in Fig. 1. All films had no secondary phase and were highly (002)-oriented irrespective of substrate. Figure 2 shows the pole figures measured at (103) plane for the as-deposited films on sapphire and fused silica substrates. The pole figure of the ZnO and AZO films on sapphire substrate shows six equivalent peaks, indicating that the films were ordered within a planar direction. However, the ZnO and AZO films grown on fused silica did not have six peaks, but formed a circle. The films on fused silica substrate were not ordered within the plane. These results, combined with the θ–2θ XRD spectrum, indicate that the films on sapphire and fused silica were epitaxial and textured polycrystalline films, respectively. In order to estimate a degree of grain ordering in out of plane, we measured the rocking curves of the films for the (002) peak. The measured values of the full-width at half maximum (FWHM) of the rocking curve are summarized in Table 1. The FWHM of the rocking curve indicates the angle of the c-axis for ZnO films compared to the normal direction of the substrate. A lower FWHM value means a more parallel c-axis relative to the direction of the substrate normal in ZnO film. In Table 1, the FWHM of the films on sapphire substrate is ~0.9–1.2 degrees, but that on fused silica is ~4.06.7 degrees. The films on the fused silica substrate had a larger FWHM of the rocking curve for c-axis than that of epitaxial films on the sapphire substrate. Figure 3 is a schematic diagram describing the grain arrangement of the

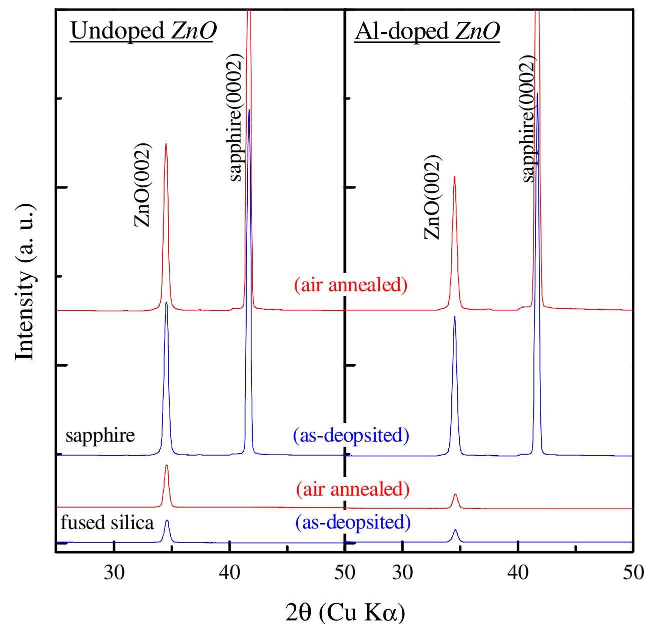

Fig. 1 XRD spectrum of undoped and Al-doped ZnO films on sapphire (*red line*) and fused silica (*blue line*) before and after the air annealing

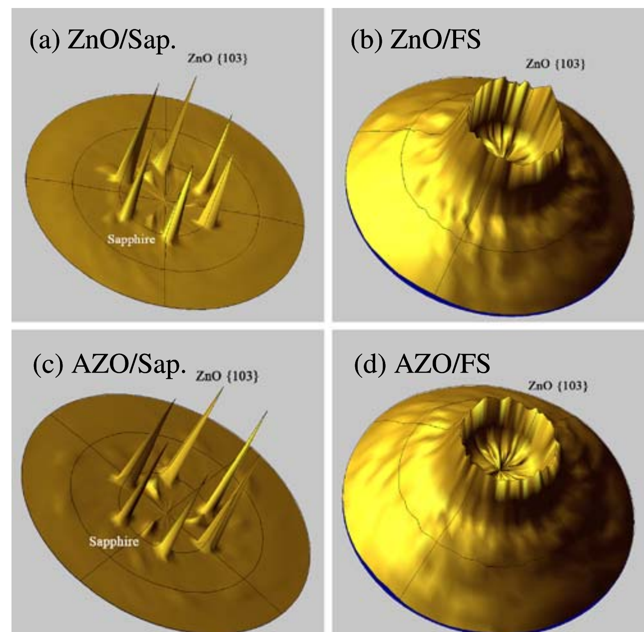

Fig. 2 Pole figure of undoped and Al-doped ZnO films on sapphire and fused silica

Table 1 FWHM of rocking curves of the ZnO and AZO films on sapphire (Sap.) and fused silica (FS) substrates before and after air annealing

	As-deposited films	Air annealed films
ZnO/Sap.	1.0	0.9
ZnO/FS	5.5	4.0
AZO/Sap.	1.1	1.2
AZO/FS	6.7	6.1

thin ZnO and AZO films on sapphire and fused silica substrates from the results of the above pole figure and rocking curve. Figure 3 shows that the textured polycrystalline films on fused silica had high-angle twist and tilt grain boundaries, while the epitaxial films on sapphire had low-angle grain boundaries. In addition, it could be concluded from the results in Table 1 that air annealing influenced only the crystal structure of the polycrystalline ZnO and AZO films on fused silica substrate, while that of the epitaxial films on the sapphire substrate was nearly unchanged after air annealing.

Figure 4 shows the resistivity, mobility, and carrier concentration of the as-deposited and air annealed ZnO and AZO films. The resistivity of as-deposited ZnO films on sapphire and fused silica substrates were 2.30×10^{-2} and 3.71×10^{-2} Ω cm, respectively. The difference in the resistivity between epitaxial and polycrystalline ZnO films was attributed to their mobility. The mobility of the epitaxial ZnO films was higher, 53 cm^2/V-S, than that, 33 cm^2/V-S, of the polycrystalline ZnO film, although the carrier concentrations of both films were equal, 5.2×10^{18} cm^{-3}. Grain boundary density and surface roughness were similar between the epitaxial and polycrystalline ZnO or AZO films according to AFM analysis (not shown here). Therefore, the difference in mobility might be attributed to the high-angle grain boundary. In general, the mobility of ZnO is a function of carrier concentration [14]. However, another variable factor on mobility exists because the carrier concentration of two films was identical. M. Brikholz et al. insisted that high-angle grain boundaries in textured polycrystalline ZnO films have a larger density of electronic defects and of active scattering centers for charge carriers than low-angle grain boundaries [15]. According to their suggestion, the low mobility of the polycrystalline ZnO film could be explained by the high-angle grain boundaries in the film.

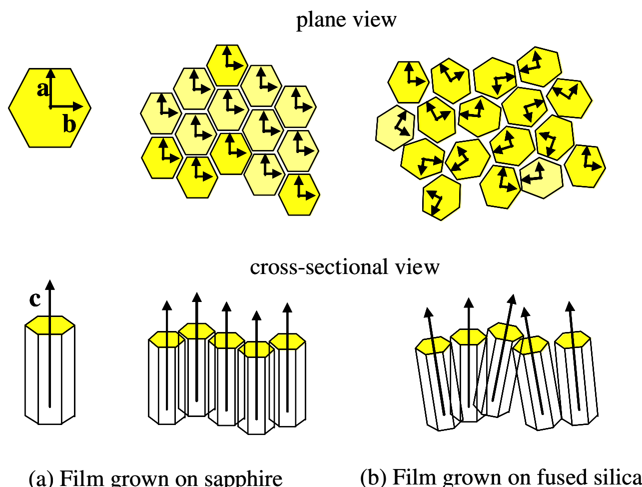

Fig. 3 Schematic diagram about arrangement of grains in the ZnO and AZO films on (**a**) sapphire and (**b**) fused silica substrates

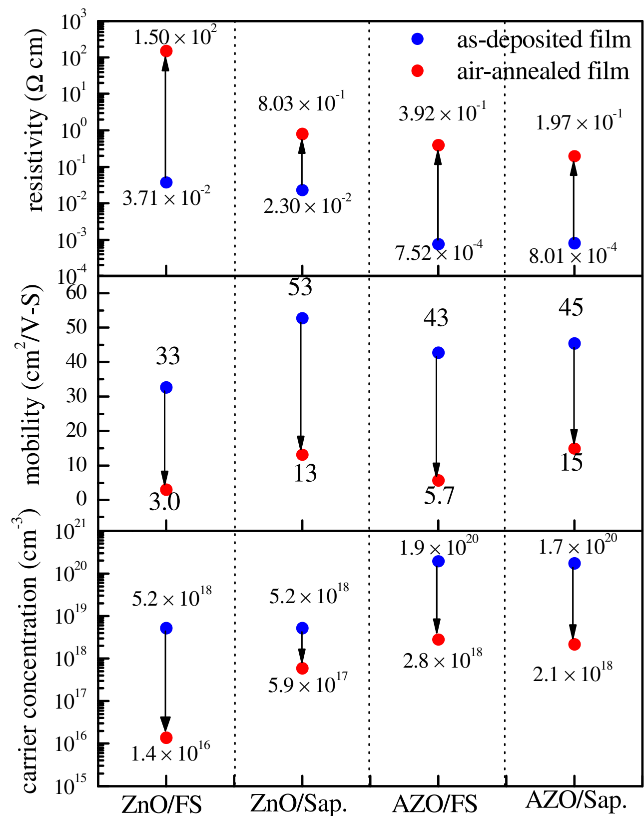

Fig. 4 Resistivity, Hall mobility, and carrier concentration of the ZnO and AZO films on sapphire (Sap.) and fused silica (FS) substrates before and after the air annealing

The air-annealed epitaxial and polycrystalline ZnO films had high resistivity values, 8.03×10^{-1} and 1.50×10^{2} Ω cm, respectively. The remarkable difference in resistivity between the air annealed epitaxial and polycrystalline ZnO films was due mainly to the carrier concentration of the epitaxial and polycrystalline ZnO films, 5.9×10^{17} and 1.4×10^{16} cm^{-3}, respectively. Undoped ZnO is an n-type semiconductor due to intrinsic defects, such as oxygen vacancies and zinc interstitials, which acted as donors [16, 17]. The air annealing process compensated for such defects so that the carrier concentration decreased. The reason why the carrier concentration of the polycrystalline ZnO film decreased more than that of the epitaxial ZnO

film was not clear. However, there was a significant difference in the FWHM of rocking curves between epitaxial and polycrystalline ZnO films, as shown in Table 1. As mentioned above, the polycrystalline ZnO film had high-angle twist and tilt grain boundaries. The intrinsic defects in ZnO film diffused to the grain boundaries during air annealing. The diffused intrinsic defects might be favorably compensated at a high-angle grain boundary by oxygen atoms compared to the low-angle grain boundary in the epitaxial film.

Al-doped ZnO (AZO) is an extrinsic n-type semiconductor. The extra electrons introduced, when an Al atom is substituted for a Zn atom by Eq. 1, are dominant carriers in the AZO film [18].

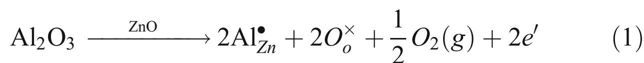

$$Al_2O_3 \xrightarrow{ZnO} 2Al^{\bullet}_{Zn} + 2O^{\times}_{o} + \frac{1}{2}O_2(g) + 2e' \quad (1)$$

As shown in Fig. 1, the Al atoms in epitaxial and polycrystalline AZO films were well doped without any secondary phase. In addition, both films have a high carrier concentration of 1.9×10^{20} and 1.7×10^{20} Ω cm, indicating that Al atoms were adequately accommodated in the ZnO matrix. Although the epitaxial and polycrystalline AZO films had different grain boundaries, the as-deposited films showed nearly identical electrical properties in Fig. 4. We inferred from the similar carrier concentrations in the two films that the doping of Al atoms into ZnO was not influenced by the formation of high- or low-angle grain boundaries during film growth. The mobilities of the epitaxial and the polycrystalline AZO films were also similar; 45 and 43 cm^2/V-S, respectively. When ZnO films have high carrier concentrations, it is commonly accepted that the mobility of polycrystalline ZnO films is limited mainly by intra-grain scattering, while grain boundary scattering is less effective [15]. V. Bhosle et al. also reported that mobility can be understood by electrical transport through a potential barrier (Φ_B) at grain boundaries in polycrystalline Ga-doped ZnO films [19]. They reported that the barrier height, Φ_B, and carrier concentration, n, are related by Eq. 2

$$\Phi_B = \frac{eQ^2}{8\varepsilon_r\varepsilon_0 n} \quad (2)$$

where Q is the electric charge trapped at the grain boundaries, ε_r is the relative dielectric constant, and ε_r is permittivity at vacuum. In addition, the activated mobility, μ, is represented by Eq. 3

$$\mu = \mu_0 \exp\left(-\frac{\Phi_B}{kT}\right) \quad (3)$$

where μ_0 is characteristic mobility.

According to Eqs. 2 and 3, the barrier height decreases with increased carrier concentration, and the barrier height becomes negligible above a critical value. From the above discussion, it was inferred that the scattering by high-angle grain boundaries in the polycrystalline AZO film was negligible at the carrier concentration used, 1.9×10^{20} cm^{-3}. Therefore, mobilities of the as-deposited epitaxial and polycrystalline AZO films were almost identical, and the resistivity of both films was also similar, although the two films had different grain boundaries.

However, air-annealed AZO films showed a difference in resistivity between the epitaxial and polycrystalline films. This difference was attributed to the difference in mobility between the epitaxial AZO films, 15 cm^2/V-S, and polycrystalline AZO films, 5.7 cm^2/V-S, as shown in Fig. 4. As mentioned above, the role of the grain boundaries was important to electrical transport at low carrier concentrations in the polycrystalline semiconductor. In particular, the barrier height at the high-angle grain boundaries was not negligible at the low carrier concentration used because the high-angle grain boundaries had a larger density of electronic defects and active scattering centers for charge carriers than low-angle grain boundaries. It was also interesting that the air annealed AZO films had nearly identical carrier concentrations in contrast to the ZnO films. The difference between the AZO and ZnO films was attributed to a source of dominant electrons for the n-type semiconductor. While the Al atoms substituted for Zn atoms played a dominant role in the formation of an extrinsic n-type

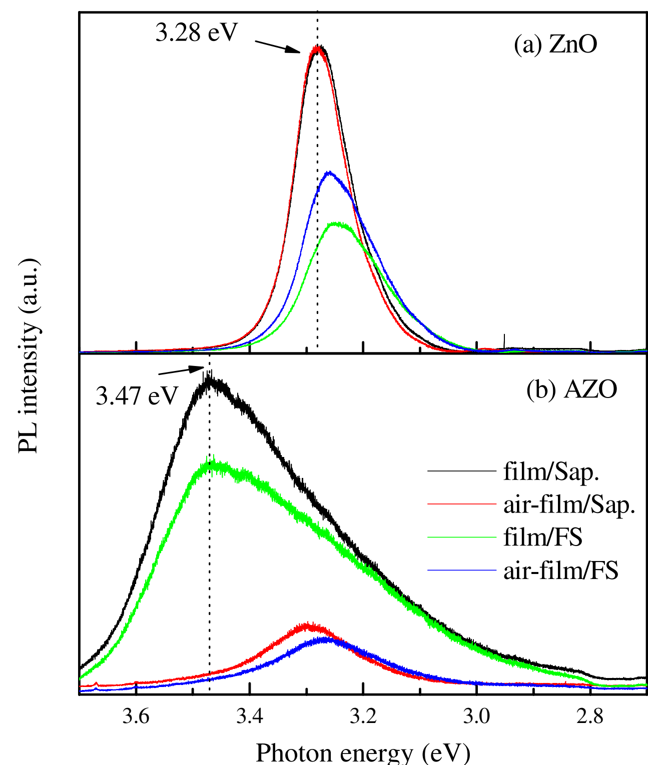

Fig. 5 Photoluminescence of the (**a**) ZnO and (**b**) AZO films on sapphire (Sap.) and fused silica (FS) substrates before and after the air annealing

semiconductor in the AZO films, the intrinsic defects, such as oxygen vacancies and zinc interstitials, were dominant factors for the formation of the intrinsic n-type semiconductor in ZnO films. During air annealing, the intrinsic defects would readily diffuse to the grain boundary compared to the Al atom bound to oxygen in the AZO film. Because the intrinsic defects were not dominant dopants in AZO films, the compensation of the intrinsic defects, such as oxygen vacancies and zinc interstitials, might not result in different carrier concentrations between high- and low-angle grain boundaries.

Figure 5 shows the near band edge (NBE) emission in photoluminescence spectra of the ZnO and AZO films at room temperature. While the as-deposited epitaxial ZnO film showed NBE emission with a high intensity at 3.28 eV, the as-deposited polycrystalline ZnO films showed lower NBE emission intensities and red shifting. Both the as-deposited epitaxial and polycrystalline AZO films had a broad NBE emission at 3.47 eV due to a Stokes shift caused by the random distribution of doping impurities [20]. The NBE emission of the air-annealed epitaxial film was not changed, but the NBE emission was improved in the polycrystalline case. This observation was due to the alignment of the polycrystalline ZnO film with the *c*-axis during air annealing, but the epitaxial ZnO films were almost constant. Both of the air-annealed AZO films had a NBE emission peak with low intensity at 3.30 eV. A non-radiative transition trap center in the AZO films would be introduced during air annealing irrespective of grain boundaries. A study in the introduced non-radiative transition trap center is in progress.

4 Conclusion

Undoped and Al-doped (1.6%) ZnO thin films were grown on (0001) sapphire and fused silica substrates using a pulsed laser deposition technique. Thin ZnO films were grown epitaxially with a low-angle grain boundary on a sapphire substrate, while they exhibited a polycrystalline nature with a textured structure on a fused silica substrate. The high-angle grain boundaries favorably offer sites for the compensation of intrinsic defects, such as oxygen vacancies and zinc interstitials, during air annealing compared to the low angle grain boundaries. The near band edge emissions in AZO films show that non-radiative transition trap centers are introduced in the AZO films irrespective of grain boundaries. Differences in compensational behaviors between intrinsic and extrinsic defects in AZO films at low- and high-angle grain boundaries during air annealing is a foundational result for the study of the thermal stability of ZnO-related TCO.

Acknowledgements This work was supported by the Korea Science and Engineering Foundation (KOSEF) grant funded by the Korea government (MOST) (R01-2007-000-11075-0) (RIAM).

References

1. Ü. Özgür, Y.I. Alivov, C. Liu, A. Teke, M.A. Reshchikov, S. Doğan, V. Avrutin, S.J. Cho, H. Morkoc, J. Appl. Phys. **98**, 041301 (2005)
2. E.C. Look, D.C. Reynolds, J.R. Sizelove, R.L. Jones, C.W. Litton, G. Cantwell, W.C. Harsch, Solid State Commun., **105**, 399 (1998)
3. Miyamoto, M. Sano, H. Kato, T. Yao, Jpn. J. Appl. Phys. **Part 2 41**, L1203 (2002)
4. A.C. Rastogi, S.B. Desu, P. Bhattacharya, R.S. Katiyar, J. Electroceram. **13**, 345 (2004)
5. A. Teke, Ü. Özgür, S. Doğan, X. Gu, H. Morkoc, B. Nemeth, J. Nause, H.O. Everitt, Phys. Rev. B **70**, 195207 (2004)
6. K.H. Kim, K.C. Park, D.Y. Ma, J. Appl. Phys. **81**, 7764 (1997)
7. N. Malkomes, M. Vergöhl, B. Szyszka, J. Vac. Sci. Technol. A **19**, 414 (2000)
8. T. Makino, K. Tamura, C.H. Chia, Y. Segawa, M. Kawasaki, A. Ohtomo, H. Koinuma, Phys. Rev. B **65**, 121201 (2002)
9. A. Tsukazaki, A. Ohtomo, T. Onuma, M. Ohtani, T. Makino, M. Sumiya, K. Ohtani, S.F. Chichibu, S. Fuke, Y. Segawa, H. Ohno, H. Koinuma, M. Kawasaki, Nat. Mater. **4**, 42 (2005)
10. F.K. Shan, Z.F. Liu, G.X. Liu, W.J. Lee, G.H. Lee, I.S. Kim, B.C. Shin, Y.S. Yu, J. Electroceram. **13**, 189 (2004)
11. H. Kim, J.S. Horwitz, S.B. Qadri, D.B. Chrisey, Thin Solid Films **420**, 107 (2002)
12. J. Mass, P. Bhattacharya, R.S. Katiyar, Mater. Sci. Eng. B **103**, 9 (2003)
13. F.-J. Haug, Zs. Feller, H. Zogg, A.N. Tiwari, C. Vignali, J. Vac. Sci. Technol. A **19**, 171 (2001)
14. G. Heiland, E. Mollow, F. Stockmann, Solid State Phys. **8**, 191 (1959)
15. M. Birkholz, B. Selle, F. Fenske, W. Fuhs, Phys. Rev. **68**, 205414 (2003)
16. J. Schoenes, K. Kanazawa, E. Kay, J. Appl. Phys. **48**, 2537 (1977)
17. G. Neumann, Phys. Status Solidi A **105**, 605 (1981)
18. J. Fan, R. Freer, J. Appl. Phys. **77**, 4795 (1995)
19. V. Bhosle, J. Narayan, J. Appl. Phys. **100**, 093519 (2006)
20. T. Makino, Y. Segawa, S. Yoshida, A. Tsukazaki, A. Ohtomo, M. Kawasaki, Appl. Phys. Lett. **85**, 759 (2004)